



Supporting Information

for *Adv. Sci.*, DOI: 10.1002/advs.202004448

Boosting reversibility of Mn-Based tunnel-structured cathode materials for sodium-ion batteries by magnesium substitution

Xun-Lu Li, Jian Bao, Yi-Fan Li, Dong Chen, Cui Ma, Qi-Qi Qiu, Xin-Yang Yue, Qin-Chao Wang and Yong-Ning Zhou**

Supporting Information

Boosting reversibility of Mn-based tunnel-structured cathode materials for sodium-ion batteries by magnesium substitution

Xun-Lu Li, Jian Bao, Yi-Fan Li, Dong Chen, Cui Ma, Qi-Qi Qiu, Xin-Yang Yue, Qin-Chao Wang^{*} and Yong-Ning Zhou^{*}

$$I_p = 2.69 \times 10^5 n^{3/2} A D^{1/2} v^{1/2} C_0 \quad \text{Equation S1}$$

Note: I_p is the peak currents of the oxidation and reduction peaks in the CV, D is the diffusion coefficient of Na^+ . n is the number of electrons per reaction species, A is the area of the electrode, C_0 is the concentration of Na^+ in the lattice, v is scan rates.

$$D_{\text{Na}^+} = R^2 T^2 / 2A^2 n^4 F^4 C^2 \sigma^2 \quad \text{Equation S2}$$

Note: R is the gas constant ($8.314 \text{ J K}^{-1} \text{ mol}^{-1}$), T is the test temperature (298 K), A is the surface area of the electrode. n is the number of the electrons per molecule during oxidization, F is the Faraday constant (96485 C mol^{-1}), C is molar concentration of Na^+ , σ is the Warburg factor ($\Omega \text{ s}^{-1/2}$) associated with Z' (real part of the cell impedance, Ω) and ω (the angular frequency, rad s^{-1})

$$Z' = R_e + R_{ct} + \sigma \omega^{-1/2} \quad \text{Equation S3}$$

Note: R_e is the resistance of the electrolyte, R_{ct} is the charge transfer resistance^[S1].

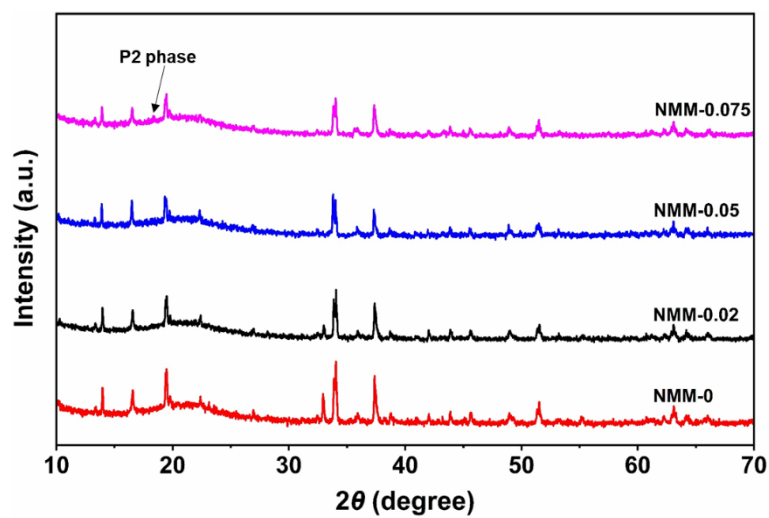


Figure S1. XRD patterns of $\text{Na}_{0.44}\text{MnO}_2$ (NMM-0), $\text{Na}_{0.44}\text{Mn}_{0.98}\text{Mg}_{0.02}\text{O}_2$ (NMM-0.02), $\text{Na}_{0.44}\text{Mn}_{0.95}\text{Mg}_{0.05}\text{O}_2$ (NMM-0.05), and $\text{Na}_{0.44}\text{Mn}_{0.925}\text{Mg}_{0.075}\text{O}_2$ (NMM-0.075).

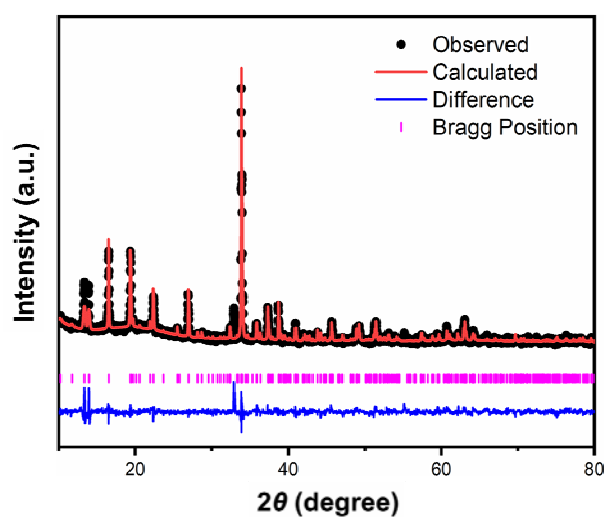


Figure S2. Rietveld refinement of the XRD pattern for $\text{Na}_{0.44}\text{MnO}_2$.

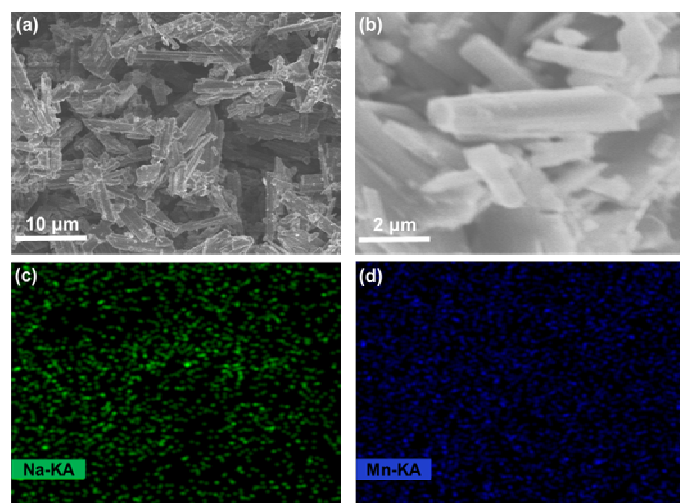


Figure S3. SEM images of a, b) NMM-0 and corresponding EDX mapping of c) Na and d) Mn.

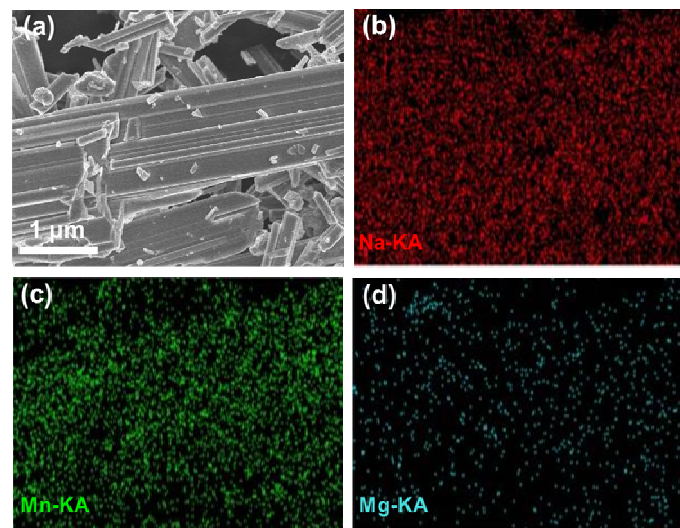


Figure S4. SEM image of a) NMM-0.05 and corresponding EDX mapping of b) Na, c) Mn and d) Mg.

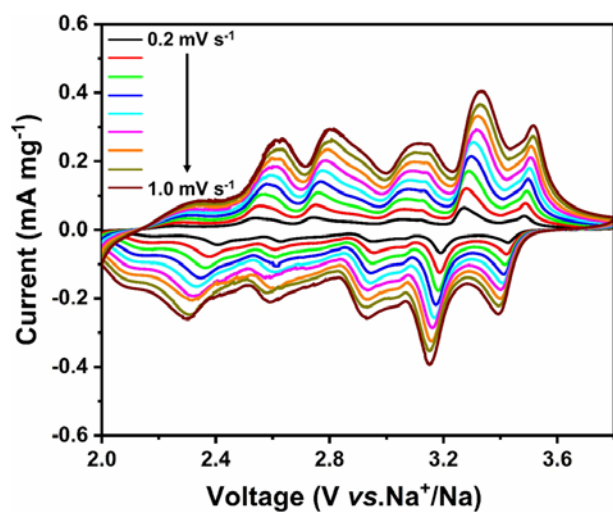


Figure S5. CV curves of NMM-0 with scan rates increasing from 0.2 to 1 mV s⁻¹.

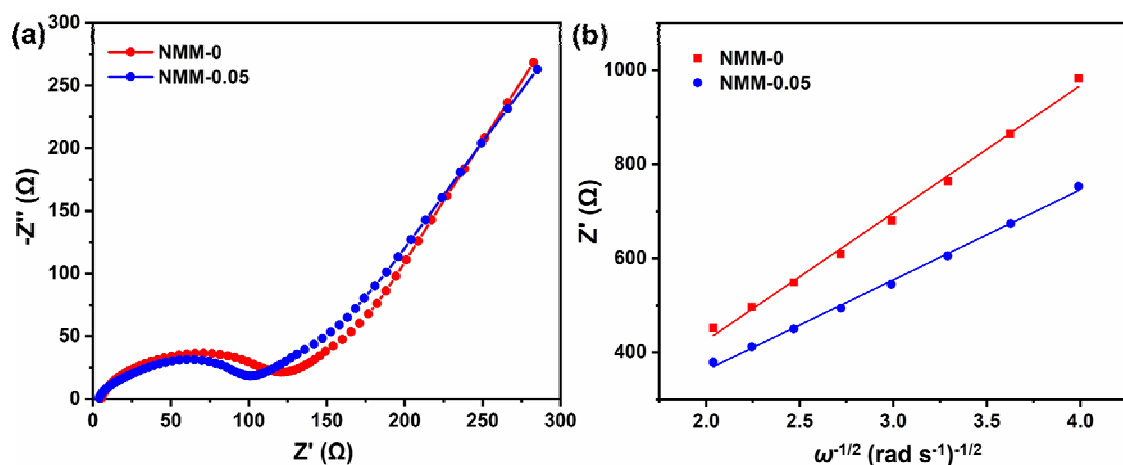


Figure S6. a) EIS spectra of NMM-0 (red) and NMM-0.05 (blue) after 20 cycles. b) Plots of Z' as a function of $\omega^{-1/2}$ in the low frequency region.

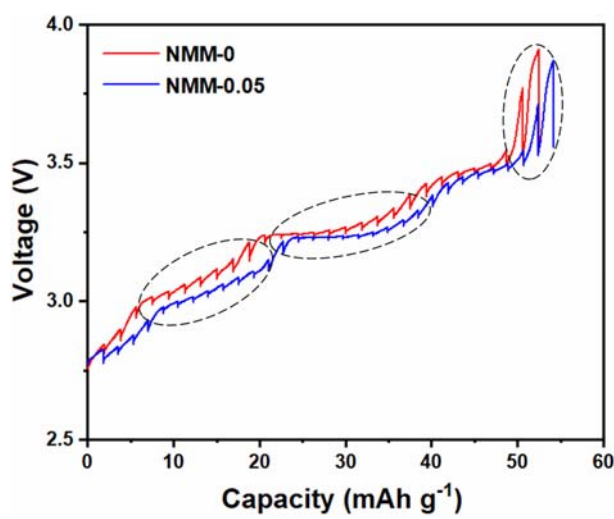


Figure S7. GITT curves of NMM-0 and NMM-0.05 in the first charge process.

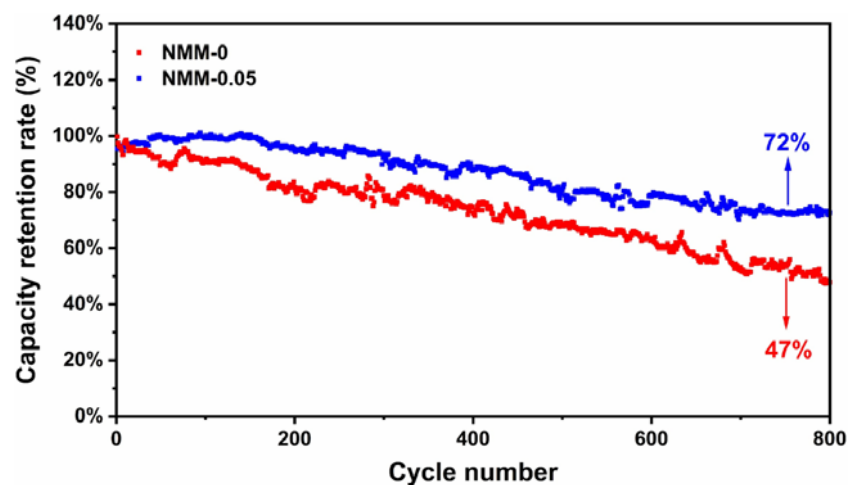


Figure S8. The capacity retention rates of NMM-0 and NMM-0.05 at 5C.

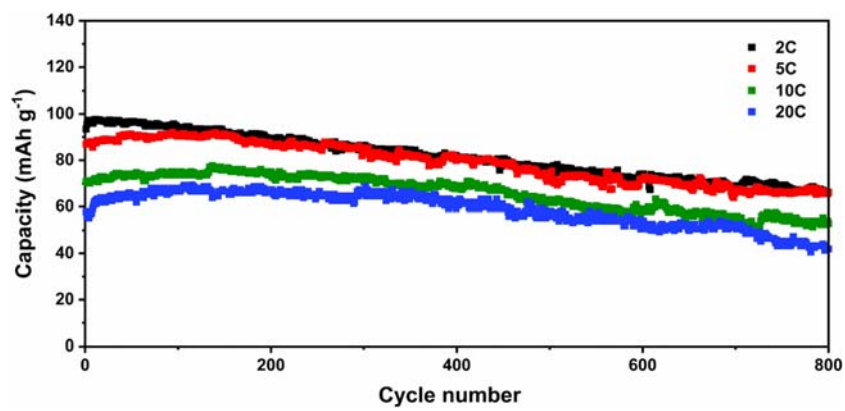


Figure S9. Long cycle performance of NMM-0.05 at 2C (black), 5C (red), 10C (green), and 20C (blue).

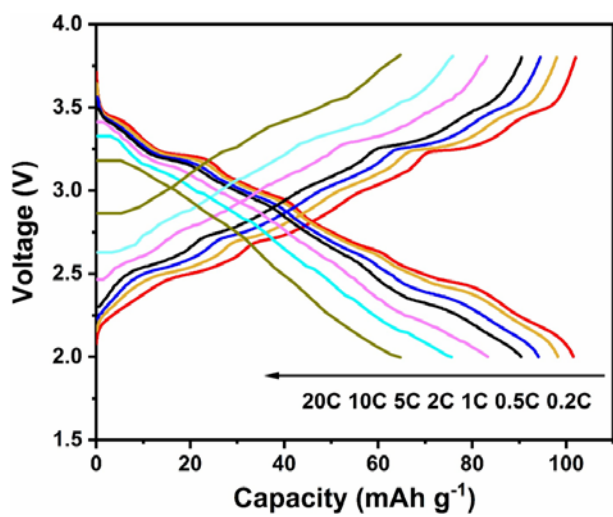


Figure S10. The galvanostatic GCD curves of NMM-0.05 between 2.0-3.8 V vs. Na^+/Na at different current densities.

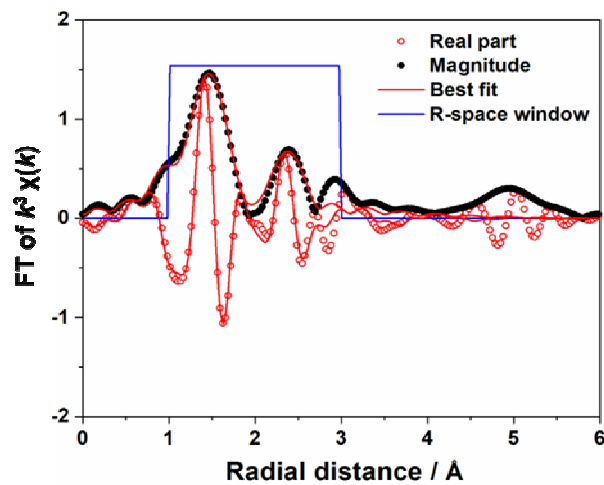


Figure S11. Least-square fits of the calculated FT-EXAFS phase and amplitude functions to the experimental EXAFS spectra for the pristine NMM-0.05.

Table S1. Crystallographic parameters of $\text{Na}_{0.44}\text{MnO}_2$ refined by Rietveld method.

Space group: <i>Pbam</i> (No. 55)						
Atom	element	Mult.	x	y	z	Occupancy
Mn1	Mn^{4+}	2	0	0.5	0	1
Mn2	Mn^{3+}	4	0.3570	0.0934	0.5	1
Mn3	Mn^{4+}	4	0.0350	0.1005	0	1
Mn4	Mn^{4+}	4	0.3490	0.3067	0.5	1
Mn5	Mn^{3+}	4	0.0260	0.3080	0	1
Na6	Na^+	4	0.2010	0.1890	0	1
Na7	Na^+	4	0.2960	0.4090	0.5	1
Na8	Na^+	4	0.1240	0.0038	0	1
O9	O^{2-}	4	0.3540	0.0020	0.5	1
O10	O^{2-}	4	0.2600	0.0930	0	1
O11	O^{2-}	4	0.0660	0.1920	0.5	1
O12	O^{2-}	4	0.5290	0.1830	0.5	1
O13	O^{2-}	4	0.1790	0.3020	0.5	1
O14	O^{2-}	4	0.3920	0.3017	0	1
O15	O^{2-}	4	0.2300	0.4000	0	1
O16	O^{2-}	4	0.5140	0.0870	0	1
O17	O^{2-}	4	0.4850	0.4100	0.5	1

$a=9.100(6)$ $b=26.394(5)$ $c=2.828(7)$ $V=679.4(9)$ $R_p=1.5\%$ $R_{wp}=2.53\%$

Table S2. Crystallographic parameters of $\text{Na}_{0.44}\text{Mn}_{0.95}\text{Mg}_{0.05}\text{O}_2$ refined by Rietveld method.

Space group: <i>Pbam</i> (No. 55)						
Atom	element	Mult.	x	y	z	Occupancy
Mn1	Mn^{4+}	2	0	0.5000	0	1
Mn2	Mn^{3+}	4	0.5130	0.0533	0.5	1
Mn3	Mn^{4+}	4	0.0297	0.1006	0	1
Mn4	Mn^{4+}	4	0.3570	0.3050	0.5	1
Mg5	Mg^{2+}	4	0.0380	0.2956	0	0.45
Mn5	Mn^{3+}	4	0.0380	0.2956	0	0.55
Na6	Na^+	4	0.2460	0.2058	0	1
Na7	Na^+	4	0.1980	0.3878	0.5	1
Na8	Na^+	4	0.1360	0.0200	0	1
O9	O^{2-}	4	0.1790	0.0030	0.5	1
O10	O^{2-}	4	0.2550	0.0912	0	1
O11	O^{2-}	4	0.1240	0.1928	0.5	1
O12	O^{2-}	4	0.3880	0.2173	0.5	1
O13	O^{2-}	4	0.0950	0.2925	0.5	1
O14	O^{2-}	4	0.3090	0.2940	0	1
O15	O^{2-}	4	1.5270	0.7028	0	1
O16	O^{2-}	4	0.3510	0.1290	0	1
O17	O^{2-}	4	0.4160	0.4134	0.5	1
$a=9.082(3)$ $b=26.432(5)$ $c=2.824(8)$ $V=678.16(4)$ $R_p=3.48\%$ $R_{wp}=4.60\%$						

Table S3. EDX results of NMM-0.

Element	Series	Atom ratio [at%]	Deviation [%]
Na	K	31.48	0.92
Mn	K	68.52	0.92

Table S4. EDX results of NMM-0.05.

Element	Series	Atom ratio [at%]	Deviation [%]
Na	K	32.67	2.0
Mn	K	63.52	1.5
Mg	K	3.81	0.4

Table S5. ICP results of the synthesized $\text{Na}_{0.44}\text{Mn}_{0.95}\text{Mg}_{0.05}\text{O}_2$.

Na	Mn	Mg
0.441	0.952	0.048

Table S6. D_{Na^+} values of NMM-0 and NMM-0.05 at the 20th cycle and 80th cycle, respectively.

Sample	20 th D_{Na^+} ($\text{cm}^2 \text{s}^{-1}$)	80 th D_{Na^+} ($\text{cm}^2 \text{s}^{-1}$)
NMM-0	7.314×10^{-11}	8.660×10^{-11}
NMM-0.05	1.386×10^{-10}	5.468×10^{-10}

Table S7 Electrochemical performance comparison of NMM-0.05 with other tunned-structured cathode materials for sodium-ion batteries.

Samples	Specific capacity (mAh g ⁻¹ @C)	Rate capability (mAh g ⁻¹ @C)	Cycling stability (%@cycle No./C)	Voltage range (V)	Ref.
Na _{0.61} [Mn _{0.27} Fe _{0.34} Ti _{0.39}]O ₂	98@0.1	43@1	90@100/0.2	2.6~4.2	[S2]
Na _{0.66} [Mn _{0.66} Ti _{0.34}]O ₂	74@0.1	-	86@400/0.1	2.5~3.9	[S3]
Na _{0.44} MnO ₂ nanofiber	118@0.42	69.5@10	67@140/0.42	1.5~4.0	[S4]
Na _{0.5} MnO ₂	115@0.1	100@2	95@30/0.33	2.0~4.0	[S5]
Na _{0.66} [Mn _{0.66} Ti _{0.34}]O _{1.94} F _{0.06}	97@0.2	65@20	87@1000/2	1.5~3.8	[S6]
NMM-0.05	105@0.2	60@30	72@800/5	2.0~3.8	This work

Table S8. Evolution of Mn K-edge EXAFS structural parameters at various states for NMM-0.05.

Samples	Path	r / Å	$\sigma^2 / 10^{-3} \text{ Å}^2$	$\Delta E / \text{eV}$	R
Pristine	Mn-O	1.892 ± 0.076	1.232 ± 1.694	-1.922 ± 2.577	0.001
	Mn-TM	2.786 ± 0.099	9.202 ± 1.857	-14.654 ± 3.564	
Fully charged	Mn-O	1.874 ± 0.075	0.336 ± 0.800	-0.075 ± 1.042	0.001
	Mn-TM	2.762 ± 0.059	5.838 ± 0.722	-7.770 ± 1.498	
Fully discharged	Mn-O	1.902 ± 0.065	1.435 ± 2.375	-0.367 ± 4.144	0.001
	Mn-TM	2.821 ± 0.124	10.402 ± 3.476	-18.602 ± 8.730	

r: bond length; σ^2 : Debye-Waller factor (disorder); ΔE : inner shell potential shift; R: R-factor

Table S9. Atom population analysis of NMM-0.

Atom	Number	s	p	d	Total
Mn	1	0.58	0.52	5.23	6.33
Mn	2	0.58	0.52	5.23	6.33
Mn	3	0.59	0.46	5.2	6.25
Mn	4	0.53	0.51	5.24	6.28
Mn	5	0.59	0.46	5.2	6.25
Mn	6	0.53	0.51	5.24	6.28
Mn	7	0.59	0.46	5.2	6.25
Mn	8	0.53	0.51	5.24	6.28
Mn	9	0.59	0.46	5.2	6.25
Mn	10	0.53	0.51	5.24	6.28
Mn	11	0.59	0.53	5.31	6.44
Mn	12	0.61	0.46	5.19	6.25
Mn	13	0.59	0.53	5.31	6.44
Mn	14	0.61	0.46	5.19	6.25
Mn	15	0.59	0.53	5.31	6.44
Mn	16	0.61	0.46	5.19	6.25
Mn	17	0.59	0.53	5.31	6.44
Mn	18	0.61	0.46	5.19	6.25

Table S10. Atom population analysis of NMM-0.05.

Atom	Number	s	p	d	Total
Mn	1	0.63	0.28	5.5	6.42
Mn	2	0.63	0.28	5.5	6.53
Mn	3	0.63	0.28	5.5	6.41
Mn	4	0.63	0.28	5.5	6.51
Mn	5	0.63	0.28	5.5	6.37
Mn	6	0.63	0.28	5.5	6.51
Mn	7	0.55	0.36	5.37	6.29
Mn	8	0.58	0.38	5.37	6.32
Mn	9	0.62	0.23	5.54	6.39
Mn	10	0.57	0.37	5.4	6.35
Mn	11	0.58	0.45	5.42	6.45
Mn	12	0.57	0.36	5.4	6.33
Mn	13	0.58	0.41	5.38	6.36
Mn	14	0.62	0.38	5.37	6.37
Mn	15	0.61	0.48	5.47	6.55
Mn	16	0.58	0.38	5.43	6.4
Mn	17	0.59	0.48	5.45	6.51

References

- [S1] J. G. Duan, C. Wu, Y. B. Cao, K. Du, Z. D. Peng, G. R. Hu, *Electrochim. Acta* **2016**, 221, 14.
- [S2] S. Y. Xu, Y. S. Wang, L. B. Ben, Y. C. Lyu, N. N. Song, Z. Z. Yang, Y. M. Li, L. Q. Mu, H. T. Yang, L. Gu, Y. S. Hu, H. Li, Z. H. Cheng, L. Q. Chen, X. J. Huang, *Adv. Energy Mater* **2015**, 5, 1501156.
- [S3] Y. S. Wang, L. Q. Mu, J. Liu, Z. Z. Yang, X. Q. Yu, L. Gu, Y. S. Hu, H. Li, X. Q. Yang, L. Q. Chen, X. J. Huang, *Adv. Energy Mater* **2015**, 5, 1501005.
- [S4] B. Fu, X. Zhou, Y. P. Wang, *J. Power Sources* **2016**, 310, 102.
- [S5] K. Y. Shen, M. Lengyel, L. Wang, R. L. Axelbaum, *MRS Commun* **2017**, 7, 74.
- [S6] Q. C. Wang, Q. Q. Qiu, N. Xiao, Z. W. Fu, X. J. Wu, X. Q. Yang, Y. N. Zhou, *Energy Storage Mater* **2018**, 15, 1.